

Design and Analysis of a PM Vernier Machine Considering the Effects of Flux Modulation and Core Losses

Byungtaek Kim, *Member, IEEE*

Department of Electrical Engineering, Kunsan National University, Gunsan, 80305 Korea, btkim@kunsan.ac.kr

This study presents the effects of flux modulation in a PM vernier motor on its core flux density and core losses as well as the basic performance characteristics such as torque and power factor. The complicated flux densities of air gap, teeth and yokes due to modulation effects are analytically calculated with the accurate air gap harmonic permeance functions. By using the derived flux density equations, a PM vernier motor is designed to have a common level of yoke flux density. To verify the analytically predicted characteristics, the flux distributions and iron losses in core parts are analyzed through time-step FE simulations. The both numerically and analytically obtained results are compared, and also evaluated against those of a conventional PM motor.

Index Terms—Core losses, finite element method, flux modulation, permanent magnet, vernier motor

I. INTRODUCTION

THROUGH DEVELOPMENT for more than 50 years, the characteristic performances of the brushless PM motors are approaching their limits. Consequently, there are strong needs for new motors with higher power density, and the PM vernier machine is being actively studied as an alternative [1]-[3]. This unique PM motor utilizes an extra flux due to magnetic modulation as well as the common PM flux [1]. Owing to this effect, it can produce much higher back EMF than a general PM motor, thus increasing power density, as has been reported in recent studies [1]-[2]. As is well known, in order to establish the flux modulation effects, special combinations of slots/magnets should be satisfied, and they commonly require much more number of PMs than that of a conventional PM machine. Generally, the thicknesses of yoke and teeth of a PM machine are proportional to the flux of a PM-pole, and the flux is inversely proportional to the number of PMs. But this is not exactly true for a vernier PM machine due to the additional modulated flux apart from the common flux of PMs. Thus, the flux distribution in the machine is more complicated and should be considered in core design. A few studies have dealt with the core losses for a specified model, however, without design considerations or comparison with the conventional ones [3].

In this study, the air gap flux distribution including the modulation flux are expressed in analytical forms and the yoke and tooth fluxes are estimated. By using the derived equations, the width of yoke of a PM vernier motor is determined so as to get the common level of flux density. Regarding to the structure, the designed PM vernier and conventional motors are compared. Finally, they are analyzed with FEM including the iron losses calculation. Various characteristics such as flux densities of each part and core losses, etc. are provided and compared with the analytically predicted results and the effects of flux modulation are discussed.

II. DESIGN OF COE PARTS OF A PM VERNIER MACHINE

A. Flux Density of Core Parts

When p , Z_s and Z_r are the numbers of stator winding pole pairs, the stator slots and rotor magnet pole pairs respectively,

in order to get the vernier effects, the special condition, $Z_r Z_s = -p$ should be satisfied, while normally $Z_r = p$ for a traditional PM machine. Since $Z_s = 6pq$ where q is slots/phase/pole, the condition is alternatively given as $Z_r = p(6q-1)$. The air gap flux density B_g is the product of the MMF F_g and the specific permeance P_g of air gap. Meanwhile, the MMF F_g consists of F_{g_a} and F_{g_m} due to stator currents and rotor magnets given by (1) and (2) respectively, where θ_m is rotor angular position, F_{m1} is given as $4/\pi \cdot B_r / \mu_m \cdot g_m$ and F_{a1} is $3/\pi \cdot N_{ph} I_{ph,max} / p$ or alternatively $K_{s,r,g}$ by using the surface current density K_s and the gap radius r_g . In (3), Λ_{g0} is the average and Λ_{g1} is the 1st harmonic of air gap permeance [1]. When the angle ϕ between the both MMFs of (1) and (2) is $\pi/2$, the air gap flux density is obtained by (4), showing the modulation flux term B_{VER} utilized in the vernier machines through the special slots/poles combinations, while it is negligible in general PM machines.

$$F_{g_m}(\theta) \approx F_{m1} \cos Z_r (\theta - \theta_m) \quad (1)$$

$$F_{g_a}(\theta) \approx F_{a1} \cdot k_{w1} \cos(p\theta + \omega_e t - \phi) \quad (2)$$

$$P_g(\theta) \approx \Lambda_{g0} + \Lambda_{g1} \cos(Z_s \theta) \quad (3)$$

$$B_g(\theta) = \underbrace{\sqrt{(F_{m1} \Lambda_{g0})^2 + (0.5k_{w1} F_{a1} \Lambda_{g1})^2}}_{B_{CON}} \cos Z_r (\theta - \theta_m + \phi_1) + \underbrace{\sqrt{(0.5F_{m1} \Lambda_{g1})^2 + (k_{w1} F_{a1} \Lambda_{g0})^2}}_{B_{VER}} \cos(p\theta + Z_r \theta_m + \phi_2) + \dots \quad (4)$$

The yoke and tooth fluxes are obtained by integrating B_g of (4) over a tooth area and the 1 pole area of stator winding respectively. Since F_{m1} is much greater than F_{a1} and Λ_{g0} is also greater than Λ_{g1} , ϕ_1 and ϕ_2 in (4) are quite small values, and thus the yoke and teeth flux can be approximated as (5) and (6) by using $Z_r = p(6q-1)$. It clearly shows that the term B_{VER}/p in yoke can be considerable, so it should be taken into account when the width of yoke is designed.

$$\Phi_{yoke}(t) \approx r_g l_{stk} \left(\frac{B_{PM}}{Z_r} + \frac{B_{VER}}{p} \right) \sin Z_r (\theta_m - \phi_3) \quad (5)$$

$$\Phi_{teeth}(t) \approx 2r_g l_{stk} \sqrt{\left(\frac{B_{PM}}{Z_r} \cos \frac{\pi}{6q} \right)^2 + \left(\frac{B_{VER}}{p} \sin \frac{\pi}{6q} \right)^2} \times \sin Z_r (\theta_m - \phi_4) \quad (6)$$

B. Core Design Considering Modulation Flux

To verify the derived equations, a PM vernier motor with $p=2$, $q=1$ and $Z_r=10$ is chosen whose PM is made from NdFeB. With the given air gap diameter and magnet thickness, the values of Λ_{g0} and Λ_{g1} can be calculated, where the slot open ratio is optimally set to 0.5 by following the previous study [1], and thus the tooth width is same to the slot open. The flux of core parts can be estimated by using (4)-(6). The general specifications and the values of B_{PM}/Z_r and B_{VER}/p in (5) and (6) are listed in table I. It should be noted that B_{VER}/p is almost twice of B_{PM}/Z_r , showing that the additional flux term should be considered in determination of width of yoke.

TABLE I
SPECIFICATIONS OF THE DESIGNED PM VERNIER MOTOR

Parameter	Value	Parameter	Value
Air gap radius	200mm	Winding poles (p)	2
Stator slots	12	Magnet poles ($2Z_r$)	20
Magnet thickness	10mm	Stack length	250mm
Conductors/slot	25	Air gap length	2mm
B_{PM}/Z_r	$4.40 \cdot 10^{-4}$	B_{VER}/p	$8.36 \cdot 10^{-4}$

The width of yoke is determined so as to get the similar level of flux density, 1.2T of general electric machines. To compare characteristic performances, a conventional PM one is also designed with the same ideas, and the both motors are demonstrated in Fig. 2. It is clear the volume of vernier motor is much smaller than the conventional even though the yoke width should be increased due to the flux modulation, representing the advantage of a vernier machine.

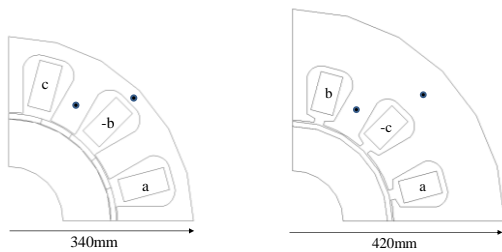


Fig. 1 Vernier and conventional motor for comparison

III. SIMULATION RESULTS

The time step FE analyses for the both motors in Fig. 1 are carried out at 500rpm at the no-load and load conditions for which the surface current density $K_s=20A/mm$ is employed. Since the electrical frequencies of both motors are substantially different due to the numbers of PMs, their iron losses should be checked carefully. The core losses are expressed by (7) in which the coefficients are estimated with the loss characteristics of Si-steel in Fig. 2 provided by manufacturer.

$$P_{iron}(B) = k_h B^2 f + k_c (Bf)^2 + k_e (Bf)^{3/2} \quad (7)$$

, where k_h , k_c , and k_e are the coefficients of hysteresis, classical eddy current, and excess eddy current losses, respectively. By using (7) and the field results from FE-simulations, the iron losses are calculated. Fig. 3 shows the various results obtained from FE analysis. The no-load back EMFs of Fig. 3(a) clearly represents the major advantage of vernier motor, higher back

EMF owing to the flux modulation. The yoke and tooth flux densities at the designated points in Fig 1 are compared in Fig. 3(b) and (c). The maximum values of yoke density are very close to 1.2T for both motors, indicating that the derived equations are very valid. The tooth flux density of the vernier motor is much lower because its tooth width is not designed with consideration for its density, but for recommended slot open ratio. Fig.3(d) shows that the average iron losses of vernier motor is about 600W, larger than 450W of the conventional due to its high operating frequency, demonstrating a drawback at high speed operation. In the full paper, the additional characteristics of torque, power factor and etc. will be provided to discuss the nature of vernier machines in detail.

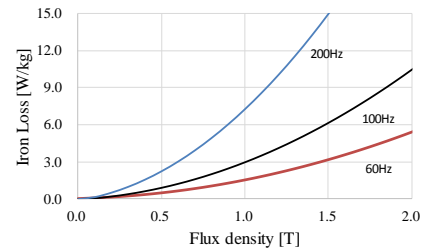


Fig. 2. Core losses per unit weight with various frequencies.

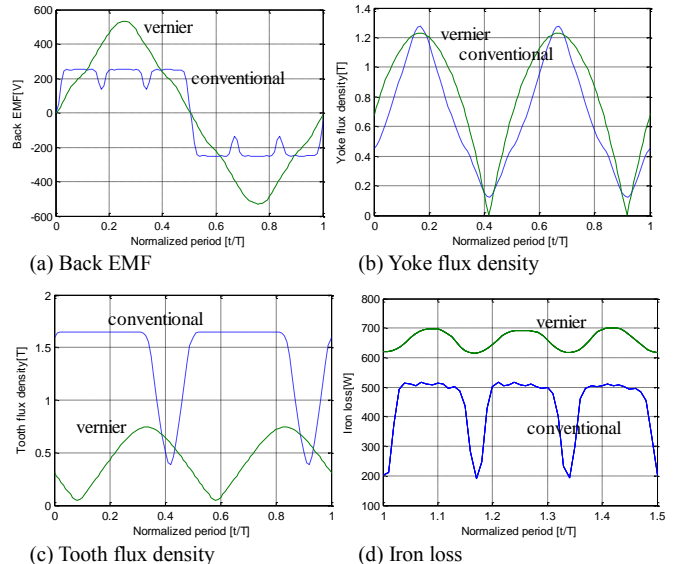


Fig. 3 Comparison of simulation results

ACKNOWLEDGEMENT

This work was supported by the Basic Science Research Program through the National Research Foundation of Korea (NRF) funded by the Ministry of Education (NRF-2016R1A6A1A03013567).

REFERENCES

- [1] B. Kim and T. A. Lipo, "Operation and Design Principles of a PM Vernier Motor", IEEE Trans. On Ind. App., Vol. 46, No. 6, 2014, pp. 3656-3663.
- [2] B. Kim and T. A. Lipo, "Analysis of a PM vernier motor with spoke structure", IEEE Trans On Ind. App., Vol. 52, No. 1, 2016, pp. 217-225
- [3] K. Okada, N. Niguchi, and K. Hirata, "Analysis of a Vernier Motor with Concentrated Windings", IEEE Trans. on Magnetics, Vol. 49, No. 5, MAY 2013, pp. 2241-2244.
- [4] X. Li, etc, "Performance Analysis of a Flux Concentrating Field Modulated Permanent Magnet Machine for Direct Drive Applications", IEEE Trans. Magnetics, Vol. 51, no. 5, 2015, pp. 2504-2506.